Geophysical Research Letters

RESEARCH LETTER
10.1029/2023GL108050

The Role of Cold Pools in Modulating Convective Organization During the MJO

Mingyue Tang[1], **Giuseppe Torri**[1], **and Naoko Sakaeda**[2]

[1]Department of Atmospheric Sciences, University of Hawai'i at Mānoa, Honolulu, HI, USA, [2]School of Meteorology, University of Oklahoma, Norman, OK, USA

Key Points:

- Enhanced Madden-Julian Oscillation (MJO) phases are associated with more organized convection than suppressed phases
- Changes in cold pool characteristics during the MJO contribute to explaining differences in convective organization
- Lower latent heat fluxes and stronger downdrafts during the active phase are responsible for the changes in cold pool characteristics

Supporting Information:

Supporting Information may be found in the online version of this article.

Correspondence to:

M. Tang,
mingyue@hawaii.edu

Citation:

Tang, M., Torri, G., & Sakaeda, N. (2024). The role of cold pools in modulating convective organization during the MJO. *Geophysical Research Letters*, *51*, e2023GL108050. https://doi.org/10.1029/2023GL108050

Received 4 JAN 2024
Accepted 30 APR 2024

Abstract In this study, we investigate the role of cold pools in modulating convective organization throughout the Madden-Julian Oscillation (MJO) life cycle using a modeling approach that combines Eulerian and Lagrangian techniques. First, we conduct a simulation using the soundings and forcing of the DYNAMO/AMIE campaign. The simulation shows a lag of several days between the precipitation rate peak time associated with MJO and the highest convective organization time. Second, to analyze the role of cold pools, we consider a series of 2-day simulations conducted at different stages of the MJO. The simulation results suggest that cold pools are larger and last longer during the mature stages of the MJO, possibly because of decreased environmental surface latent heat fluxes and stronger downdrafts. These lead to the formation of moist rings at the leading edges of cold pools, facilitating the formation of more convective cores and increasing the degree of convective organization.

Plain Language Summary Clouds typically exhibit some degree of organization and rarely exist as isolated entities. When clouds become organized, small and short-lived individual clouds can merge into larger systems that persist for much longer periods of time. Cold pools, air currents that form beneath precipitating clouds and propagate on the surface, are thought to play an important role in facilitating the formation of new clouds. In this study, we investigate the role of cold pools in the organization of convection during a phenomenon known as the Madden-Julian Oscillation (MJO). Using numerical simulations and previously defined metrics, we provide a quantitative description of cloud organization at different stages of the MJO. We then argue that within a specific region of the central Indian Ocean, there are notable changes in cloud organization and the life cycle of mesoscale convective systems. These changes occurred as the MJO transitioned from an initial to a more mature stage. Finally, we show that the size and duration of cold pools are strongly influenced by the MJO phase in which they form.

1. Introduction

The Madden-Julian Oscillation (MJO) is an eastward propagating disturbance that originates in the Indian Ocean and which repeats with a period of 30–90 days (Madden & Julian, 1971; Madden & Julian, 1972; C. Zhang, 2005). The MJO has been shown to influence weather and climate phenomena worldwide (Jones & Carvalho, 2002; Maloney & Hartmann, 2000). The envelope of the MJO is composed of mesoscale convective systems (MCSs), which in turn are made of individual clouds that organize across space and time. This organization is influenced by the environmental conditions in which clouds form, but it can also have significant effects on the larger-scale initiation and propagation of the MJO (C.-C. Chen et al., 2021; B. Chen & Mapes, 2018; Moncrieff, 2019; B. Wang et al., 2005; Yang et al., 2019). Thus, a better understanding of convective organization and its interaction with the MJO is critical in the study of the tropical atmosphere.

The role of organization in atmospheric convection has been acknowledged for many years. For example, interactions between deep convective clouds through collisions of their associated cold pools were invoked to explain the formation of new convective cells that allowed the maintenance of thunderstorms (Jeevanjee & Romps, 2015; Torri et al., 2015; Zuidema et al., 2017). Following these studies, the organization was also shown to be a key ingredient in the transition from shallow to deep convection (M. Khairoutdinov & Randall, 2006; Y. Zhang & Klein, 2010), in the life cycle of squall lines and other MCSs (Feng et al., 2012; Rotunno et al., 1988; Schlemmer & Hohenegger, 2014), and a somewhat intrinsic tendency toward which deep convective systems evolve (Wing & Emanuel, 2014). Recent evidence has shown that organization also occurs in the case of shallow convection (Bretherton & Blossey, 2017; George et al., 2023; Stevens et al., 2020).

Cold pools are one key component of deep convective systems. Formed when evaporatively cooled downdraft air enters the boundary layer, cold pools are density currents that spread along the surface while recovering their buoyancy (Droegemeier & Wilhelmson, 1985). Since the leading edge of the cold pools is characterized by positive pressure anomalies (Houze, 1994), collisions between various cold pools, or the interaction between cold pools and environmental wind shear, can lift air parcels to their level of free convection, thus facilitating the formation of new convective cells. This mechanism, called *mechanical forcing*, has been contrasted with the *thermodynamic forcing*, which is due to the thermodynamic advantage provided to parcels by the positive moisture anomalies often found at the leading edge of old cold pools (Tompkins, 2001; Torri & Kuang, 2016b). While these mechanisms, or a combination of them (Torri et al., 2015), have been invoked to explain the formation of new convective cells, recent work has questioned the role of cold pools in the life cycle of MCSs over tropical oceans (Grant et al., 2018; Lane & Moncrieff, 2015).

Convective organization has also been considered in the context of the MJO, where several authors highlighted its role in triggering new convective cells (Feng et al., 2015; Sakaeda & Torri, 2023). Even though the indices introduced to measure organization have some limitations and sometimes appear in conflict, there is evidence that different phases of the MJO are characterized by different degrees of organization (Sakaeda & Torri, 2022). While a number of factors have been hypothesized to play an important role in convective organization (Cheng et al., 2020), cold pools are recognized as a key driver of organization at any phase of the MJO.

Relatively little is known about how convective organization evolves throughout the MJO lifecycle and how cold pool properties evolve accordingly. In this work, we will address these points by exploring two questions:

- How does convective organization evolve during the MJO lifecycle?
- How do cold pools modulate convective organization during the MJO?

In Section 2, we will describe the numerical model and the simulations used for this work; in Section 3, we will present the main results, and a discussion of their implications and the conclusions will be presented in Sections 4 and 5, respectively.

2. Methods and Data

2.1. Simulations and MJO Phases

The main results of this work are obtained using the System for Atmospheric Modeling (SAM), version 6.11.2. This model solves the anelastic equations of motion and uses liquid-water static energy, total nonprecipitating, and precipitating water as thermodynamic prognostic variables (M. F. Khairoutdinov & Randall, 2003). Doubly periodic boundary conditions are used in the horizontal directions. A sponge layer is used in the upper third part of the domain to dampen gravity wave reflection. The model is run using the double-moment Morrison microphysics scheme (Morrison et al., 2005), the Smolarkiewicz' MPDATA advection scheme, the CAM3 radiation scheme, and a prognostic TKE 1.5-order closure scheme to parameterize the sub-grid effect. The model is forced using 3-hourly large-scale tendencies obtained from the Dynamics of MJO/Cooperative Indian Ocean Experiment on Intraseasonal Variability in the Year 2011 (DYNAMO/CINDY2011) northern sounding array (Johnson & Ciesielski, 2013) that this version of SAM comes equipped with. Horizontal Winds are nudged with a time scale of 3 hr, but no nudging is imposed on the temperature and moisture field.

In this paper, two kinds of simulations are used. The first encompasses the full duration of the DYNAMO campaign, from 1 October 2011 to 31 December 2011. This simulation is used to investigate the evolution of convective organization during different phases of the MJO. SAM is run with a domain measuring 256×256 km^2 in the horizontal direction. The horizontal grid spacing is 1 km in both directions. The vertical grid spacing ranges from 50 m near the surface to 500 m in the mid-to-upper troposphere, gradually becoming 1,000 m above a height of 20 km. The time step of our simulation is set to 10 s.

The second type of simulation focuses specifically on the physical mechanisms involved in convection organization. SAM is coupled with the Lagrangian Particle Dispersion Model (LPDM; Nie & Kuang, 2012; Torri et al., 2015), and three simulations are conducted, each lasting for 48 hr with a 48-hr spin-up period, which is then discarded. These simulations are started on October 10, 15, and 23, corresponding, respectively, to suppressed, growing, and enhanced phases of the MJO (Sakaeda & Torri, 2023). The simulations are initialized with 1,080 particles per model-column, randomly distributed in the pressure coordinate (Torri & Kuang, 2016b). The

horizontal grid spacing is 250 m with a domain measuring $96 \times 96 \times 27.75$ km^3. The vertical grid spacing starts at 50 m near the surface and gradually increases to 250 m above a height of 5 km. The temporal interval is 10 s, and three-dimensional outputs and particle positions are saved every 60 s. The sub-cloud layer is defined as the bottom 10 layers of the model, corresponding to a height of 618 m (Torri & Kuang, 2016a).

Since the simulations are conducted on a relatively small domain, we use a local MJO index instead of the more commonly used indices (S. Wang et al., 2015). In the 92-day simulation, a 30-day low-pass Butterworth filter (Butterworth, 1930) is applied to the outgoing longwave radiation (OLR) anomalies. The result and its time tendency are used to construct a local phase diagram similar to Riley et al. (2011) and Sakaeda et al. (2020) (see Figure S1 in Supporting Information S1). Phase 5, characterized by the minimum OLR and null tendency, represents the center of the MJO enhanced phase, while Phase 1 represents the center of the suppressed phase. Thus, the three episodes occur during phase 1–2, phase 2–3, phase 5–6 of the first MJO event. While 3 MJO cycles are observed in the long simulations, a discrepancy between observations and the model for the third event leads us to focus only on the first two (see Figure S2 in Supporting Information S1). A similar discrepancy was also noticed by other authors (S. Wang et al., 2015).

2.2. Tracking Cold Pools

Cold pool tracking is done similarly to (Torri & Kuang, 2019). First, we select cold pool cores–which are related to precipitating downdrafts–defined as regions of contiguous grid boxes in the sub-cloud layer for which the total precipitating water mixing ratio, q_p, is greater than 1.0 g kg^{-1}, and the density potential temperature anomaly with respect to the horizontal mean, θ'_ρ, is lower than -1 K. Using a breadth-first search (BFS) algorithm, we identify all the cold pool cores, and assign an identity number to those that contain more than 250 grid boxes over the entire duration of the core.

Whenever a particle injected in the sub-cloud layer by a downdraft enters a cold pool core, the particle is assigned the same identity number as the core itself. The particle maintains this identity number until it is in a grid box with non-negative buoyancy. Upon entrance into the cold pool core, each particle is also assigned a clock, and its initial position is recorded. The clock is initialized at 0 and updated every time step the particle has negative buoyancy. We then scan through each cold pool grid box that contains tracked particles and compute the distribution of clock readings and distances traveled by the particles from their initial positions. From the latter, we subtract the distance traveled because of the background winds to account for advection. Finally, the modes of these distributions are taken as an estimate of the identity number, the radius, and the age of the cold pool grid box. A representation of the evolution of the tracked cold pools is shown in Figure S3 in Supporting Information S1.

2.3. Quantifying Organization

As recently highlighted by previous studies (Biagioli & Tompkins, 2023; Cheng et al., 2018; Sakaeda & Torri, 2022; Shamekh et al., 2023), many indices have been proposed to measure convective organization, each with its strengths and limitations. In this work, we will use I_{org} (Tompkins & Semie, 2017), which compares the cumulative density function of nearest neighbor distances (NNCDF) from a cloud field with that of an equal number of randomly distributed points (NNCDF$_{random}$). The latter is given by a Weibull distribution:

$$NNCDF_{random} = 1 - \exp\left(-\lambda \pi d^2\right), \tag{1}$$

where λ is the number of points per unit area, and d is the nearest neighbor distance between randomly distributed points. I_{org} is determined by integrating the area below the curve described by (see Figure 18 of Tompkins & Semie, 2017):

$$I_{org} = \sum NNCDF(d)[NNCDF_{random}(d + \delta d/2) - NNCDF_{random}(d - \delta d/2)]. \tag{2}$$

I_{org} values range between 0 and 1, with 0.5 indicating that the clouds are randomly distributed, while larger values indicate that clouds are more organized. Following (Tompkins & Semie, 2017), we will apply I_{org} to convective updrafts. These are defined here as clusters of grid boxes with vertical velocity, w, greater than 0.75 m s^{-1} at an altitude of 3,214 m. An area of connected grid boxes satisfying this condition is identified as a cluster. Each two-

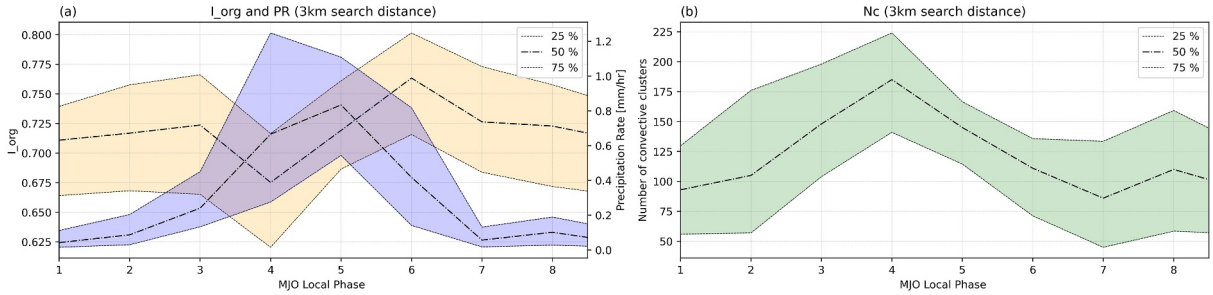

Figure 1. (a) The dash-dotted lines represent the median values of precipitation rate and I_{org} as a function of MJO phase, while the orange and blue shading represent the range between the 25th and 75th percentile of I_{org} and precipitation rate, respectively; (b) the same as (a), but representing the number of convective clusters.

dimensional cluster is then represented by its geometric centroid, which is used to calculate nearest neighbor distances (NNDs) for I_{org}.

To determine I_{org}, we will consider two grid boxes as connected if they appear within a 3-km radius of each other. The reason for this choice is that, for high enough resolutions, the turbulent nature of convective updrafts may make their two-dimensional slice appear as an inhomogeneous mixture of grid boxes with opposing signs of vertical velocity (see Figure S4 in Supporting Information S1). Thus, selecting only contiguous cells might lead us to count as separate the various components of the same updraft.

3. Results

3.1. Simulated Evolution of Cloud Organization With the MJO

The lines in Figure 1a depict the median precipitation rate and I_{org} values across different MJO phases. Shaded regions represent the range 25th–75th percentile range. Precipitation rates increase after Phase 3, with 75th (25th) percentile peaking during Phase 4 (5). Consistent with the observational analysis of Sakaeda and Torri (2022), the simulated maximum in cloud organization lags behind the precipitation rate maxima by 1–2 phases. We also examined the evolution of this quantity (Figure 1b). The plot shows that the number of convective clusters peaks during Phase 4, ahead of the I_{org} and precipitation rate maxima. Thus, convective clusters become less random while their number decreases, which is consistent with previous observations (Cheng et al., 2018; Sakaeda et al., 2020). While the selection thresholds for identifying convective points and the clustering methodology exhibit sensitivity in computing the magnitude of I_{org}, the trends of I_{org} following precipitation rate maxima demonstrate consistency.

Next, we analyze the distribution of convective clusters more closely and compute the distances between any two identified updrafts (not just their nearest neighbors). We then group these distances according to the neighboring order (e.g., nearest neighbors, next-to-nearest neighbors, next-to-next-to-nearest neighbors, etc.), and compute the distribution of distances for each order. Figure 2a presents the difference between the distances during the enhanced (Phases 5–6) and the suppressed (Phases 1–2) phases of the MJO as a function of distance (y-axis) and neighboring order (x-axis). Each distribution has been normalized to 1 before subtracting. The figure shows that the enhanced phase is associated with smaller distances between convective clusters. This is consistent with the finding that this phase is more organized (Figure 1a), particularly at higher orders.

To better understand the reasons for the changes in cluster distances with the phases of the MJO, we next consider the horizontal area of each convective cluster, a quantity that affects the minimum NND between clouds. The lines in Figure 2b show the probability distribution functions of convective cluster areas for different MJO phases. As the plot suggests, updrafts appear larger during the enhanced phases of the MJO.

Finally, as a consistency check on our findings of how MJO affects distances between updrafts, we consider the distribution of distances between any two updrafts shown in Figure 2c, without restricting to any neighboring orders. The black line represents the density function of distances in a random distribution of points and was computed by randomly distributing 10,000 points on a plane. The distribution of distances in Phase 6 has the largest departure from the random distribution, which we interpret as a sign of enhanced organization, especially

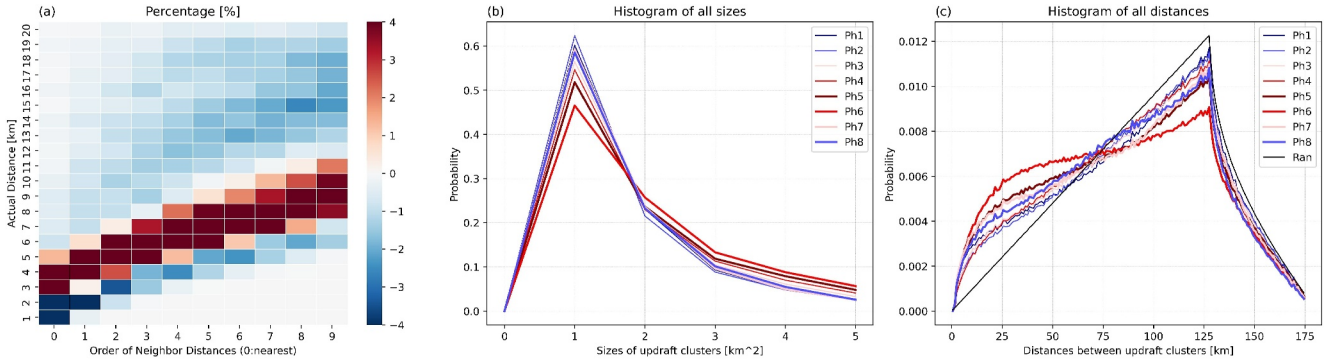

Figure 2. (a) Difference of distribution of distances by neighboring order between Phases 5–6 and Phases 1–2. (b) PDFs of sizes of the convective clusters in different MJO phases. (c) PDFs of all the distances between the cloud clusters in different MJO phases. The black line represents the distribution of 10,000 randomly distributed points, whose distances and probabilities should be linearly proportional if boundary effects are neglected.

at distances below 75 km. This is consistent with the results from Figure 1a, and it is less sensitive to the behavior of nearest neighbors, which can be a limited group to analyze.

3.2. Impacts of Cold Pools on Cloud Organization at Different MJO Phases

To examine the impact of the MJO on cold pools, we now concentrate on the 2-day SAM-LPDM simulations. Figures 3a–3c show the average surface values of cold pool specific humidity anomaly (w.r.t. the horizontal mean), q_v', as a function of cold pool radius and age. To facilitate the reading of the figure, for every value of cold pool age, we plotted the values contributed to by the first 99.99% of points counted starting from the 0-km radius. This minimized the visual interference from a few spurious points at anomalously large distances from the cold pool center that appeared at the early stages of cold pool propagation.

Results show that cold pools are much smaller during suppressed (Figure 3a) than in enhanced stages of the MJO (Figures 3b and 3c). The slopes of the outer edges of the shaded areas also suggest that cold pools propagate much more slowly during the suppressed MJO phase than the enhanced stages. Another difference between phases is the presence of anomalously high q_v' values near the leading edge of cold pools, a phenomenon often called moist patch (Drager & van den Heever, 2017; Langhans & Romps, 2015; Schlemmer & Hohenegger, 2014; Tompkins, 2001; Torri & Kuang, 2016b). This feature is particularly pronounced in the third episode, where it appears between 1 and 2 hr of cold pool birth at a distance of 20–45 km. On the other hand, for the first episode, the moist patch is much smaller and appears at earlier stages of the cold pool life cycle.

To explain the observed differences between cold pools at various MJO phases, we examine the surface fluxes. As shown in Figure S5 in Supporting Information S1, sensible heat fluxes (SHF) are much smaller than latent heat fluxes (LHF), so we will focus on the latter. Figures 4a–4c show a comparison between snapshots of surface LHF

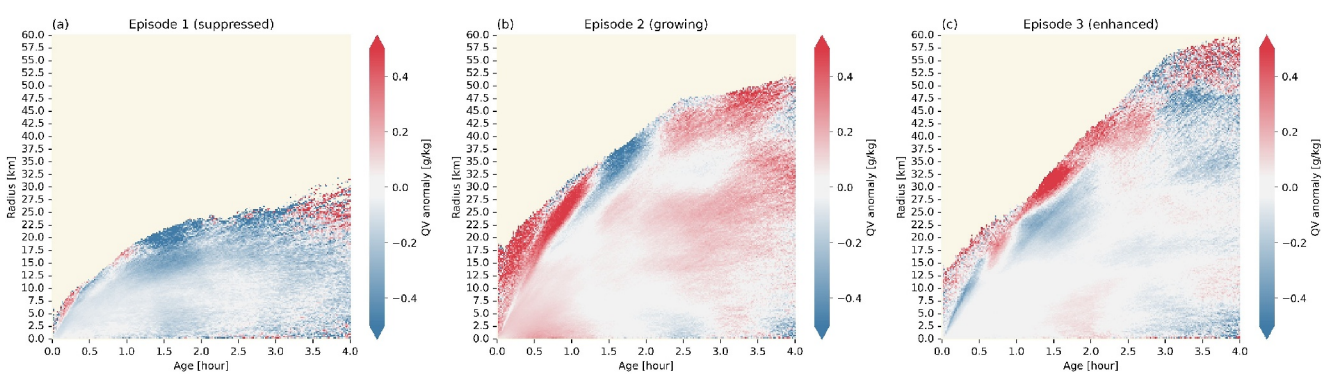

Figure 3. Cold pool-averages of surface values of q_v' during 2-day episodes in the convective suppressed (a), growing (b), and enhanced phases (c), respectively.

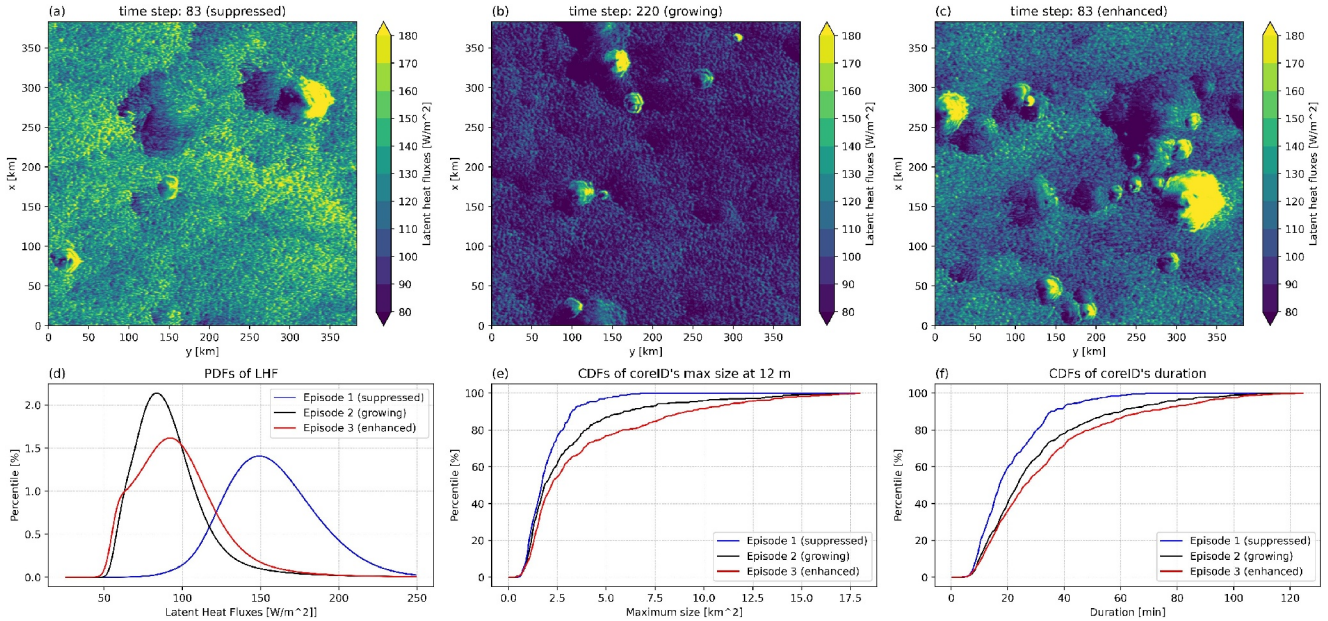

Figure 4. (a)–(c) Screenshots of surface LHFs during three 2-day rainfall episodes in the convective suppressed (a), growing (b), and enhanced (c) phases of the MJO. (d) The PDFs of surface latent heat fluxes. (e)–(f) The CDFs of the maximum size of cold pool cores related to precipitating downdrafts (e) and their duration (f). The blue, black, and red curves represent the episodes in the convective suppressed, growing, and enhanced phases, respectively.

taken during the simulated 2-day episodes. The suppressed phase (Figure 4a) shows significantly higher environmental LHF values than the other two episodes.

These differences can be appreciated in a more systematic way in Figure 4d, which shows the probability density function (PDF) of LHF at each surface spatial point for various 2-day precipitation episodes. These values are consistent with those reported by (Ruppert & Johnson, 2015). During the suppressed phase, the mode of the PDF occurs at approximately 150 W m^{-2}, twice the magnitude of the modes during the growing/enhanced phases. High LHFs above 180 W m^{-2} at the downwind side of cold pools are modulated by the combination of the background and gust winds (Figure S6 in Supporting Information S1), indicating that the asymmetric moist ring prefers to organize clouds at a distance equal to its radius rather than its diameter (Figure 2c).

Figure 4e shows a comparison between CDFs of maximum cold pool core area–a proxy for downdraft size–for the three simulated episodes. The lines in the plot show that cores in the growing (black) and enhanced (red) MJO phases are considerably bigger than in the suppressed phase (blue). This is particularly true for the larger cold pool cores in each simulation: for example, the values of the 80th percentile in the enhanced phase are almost three times as large as those in the suppressed phase.

Finally, the curves in Figure 4f represent the CDFs of cold core duration, which were determined by counting the time steps between the moment when a new cold core is identified and when no more grid cells of that cold core are found in the domain. The plots suggest that growing/enhanced MJO phases are characterized by longer-lasting cores than the suppressed phase.

4. Discussion

Cold pools are key players in the organization of convection. Their role in the shallow-to-deep transition or the life cycle of MCSs has long been acknowledged. However, less is known about their role in modulating convective organization during the MJO, a question we addressed here using a series of high-resolution numerical simulations and Lagrangian diagnostics.

Figures 1 and 2c both show that the peak in convective organization associated with the MJO lags the peak in precipitation rate. This is consistent with the findings of Sakaeda and Torri (2022), who showed similar findings using observational data. We suppose it is because the convective clouds can continuously stimulate new

convective development through specific mechanisms such as cold pool thermodynamics. Still, the establishment of these spatial connections between clouds requires time, contributing to the observed lag and maintaining the local convective system.

Our results suggest that cold pools are much larger and propagate at a higher speed during the growing and enhanced phases of the MJO compared to suppressed phases (Figures 3a–3c). They also suggest that cold pools develop stronger and wider moist patches at their edges than those in the suppressed phase. These anomalously moist areas could lead to the formation of more closely spaced convective clouds in the vicinity of the parent cloud. This could explain the increase in clustering during Phase 6 that we diagnosed using I_{org} values (Figure 1) and analysis of distances between clouds (Figure 2c). Note also that in the latter case, the relative maximum of distances, especially at Phase 6, coincides with the location of the moist patch in Figure 3c.

We attribute the diagnosed cold pool differences to differences in latent heat fluxes and downdraft characteristics. Figures 4a–4d show that there are substantial differences in LHF values across different phases of the MJO, with larger values during the suppressed phase and smaller during the growing and the mature phase. Larger LHF values likely lead to a much faster recovery of buoyancy and a significantly shorter cold pool life cycle. SHFs do not exhibit significant variations and are much smaller than LHFs.

At the same time, Figures 4e and 4f show that downdrafts during the growing and enhanced phases are larger and last longer than in the suppressed phase. The differences between MJO phases are particularly accentuated in the higher percentiles of the distributions of downdraft sizes and duration (Figures 4e and 4f).

Our results agree with previous work that showed that cold pools are important for triggering new convective cells for organizing convection (Sakaeda & Torri, 2022, 2023). At first, these findings might seem in apparent contradiction with (Grant et al., 2018), who showed that weakening/removing cold pools in numerical simulations bore no significant consequences on the propagation of MCSs over the tropical ocean. However, our results merely suggest that cold pools play a role in modulating convective organization and do not exclude other players such as gravity waves, and the impact of environmental conditions such as vertical wind shear and moisture. Following the remarks of Grant et al. (2018), gravity waves might be a key ingredient in the propagation of MCSs, while cold pools could shape convective organization at smaller spatial scales.

5. Conclusions

The organization of convective clouds is a widespread phenomenon in the Earth's atmosphere, and, through the years, it has been shown to play a critical role in many different contexts, such as the development of deep convection, the life cycle of MCSs, and even cloud-radiative feedbacks.

This work mainly focused on the evolution of convective organization across MJO phases and the role played by cold pools in modulating it. Simulations conducted using soundings and forcing collected during the DYNAMO/AMIE observational campaign show a significant change in convective organization, with the largest values during the mature stages and the lowest during the suppressed stages of the MJO. The peak in convective organization was observed to lag that in precipitation rate by one MJO phase. These findings were shown to be robust when different metrics were used to evaluate convective organization.

In order to explore the role of cold pools in modulating convective organization, a series of high-resolution 2-day simulations were conducted with an Eulerian model coupled with a Lagrangian particle model. Using a cold pool tracking algorithm, it was shown that the location of moist rings at the cold pool edges coincides with the most preferred distance between clouds. The cold pools exhibited significant differences in their characteristics, with mature MJO phases featuring larger and longer-lasting cold pools, while smaller cold pools were observed during suppressed MJO phases. These differences were explained as due to variations in surface latent heat fluxes and in downdraft characteristics. Considering these observed differences and the role of cold pools in triggering new convective cells, it was hypothesized that variations in cold pool characteristics were largely responsible for the modulation of convective organization.

Data Availability Statement

Data is available at Tang (2024) (https://doi.org/10.5281/zenodo.10939337).

Acknowledgments
We acknowledge the support by DOE through the award DE-SC0020188. We acknowledge the valuable discussions with Hrag Najarian and Zhouyu Li. The technical support and advanced computing resources from University of Hawai'i Information Technology Services–Cyberinfrastructure, funded in part by the National Science Foundation MRI award number 1920304, are also gratefully acknowledged. This is SOEST contribution number 11798. We thank two anonymous reviewers for their constructive comments.

References

Biagioli, G., & Tompkins, A. M. (2023). Measuring convective organization. *Journal of the Atmospheric Sciences*, *80*(12), 2769–2789. https://doi.org/10.1175/jas-d-23-0103.1

Bretherton, C., & Blossey, P. (2017). Understanding mesoscale aggregation of shallow cumulus convection using large-eddy simulation. *Journal of Advances in Modeling Earth Systems*, *9*(8), 2798–2821. https://doi.org/10.1002/2017ms000981

Butterworth, S. (1930). On the theory of filter amplifiers. *Wireless Engineer*, *7*(6), 536–541.

Chen, B., & Mapes, B. E. (2018). Effects of a simple convective organization scheme in a two-plume gcm. *Journal of Advances in Modeling Earth Systems*, *10*(3), 867–880. https://doi.org/10.1002/2017ms001106

Chen, C.-C., Richter, J., Liu, C., Moncrieff, M., Tang, Q., Lin, W., et al. (2021). Effects of organized convection parameterization on the mjo and precipitation in e3smv1. part I: Mesoscale heating. *Journal of Advances in Modeling Earth Systems*, *13*(6), e2020MS002401. https://doi.org/10.1029/2020ms002401

Cheng, W.-Y., Kim, D., & Rowe, A. (2018). Objective quantification of convective clustering observed during the amie/dynamo two-day rain episodes. *Journal of Geophysical Research: Atmospheres*, *123*(18), 10–361. https://doi.org/10.1029/2018jd028497

Cheng, W.-Y., Kim, D., Rowe, A., Moon, Y., & Wang, S. (2020). Mechanisms of convective clustering during a 2-day rain event in amie/dynamo. *Journal of Advances in Modeling Earth Systems*, *12*(3), e2019MS001907. https://doi.org/10.1029/2019ms001907

Drager, A. J., & Van Den Heever, S. C. (2017). Characterizing convective cold pools. *Journal of Advances in Modeling Earth Systems*, *9*(2), 1091–1115. https://doi.org/10.1002/2016ms000788

Droegemeier, K. K., & Wilhelmson, R. B. (1985). Three-dimensional numerical modeling of convection produced by interacting thunderstorm outflows. part I: Control simulation and low-level moisture variations. *Journal of the Atmospheric Sciences*, *42*(22), 2381–2403. https://doi.org/10.1175/1520-0469(1985)042<2381:tdnmoc>2.0.co;2

Feng, Z., Dong, X., Xi, B., McFarlane, S. A., Kennedy, A., Lin, B., & Minnis, P. (2012). Life cycle of midlatitude deep convective systems in a Lagrangian framework. *Journal of Geophysical Research*, *117*(D23). https://doi.org/10.1029/2012jd018362

Feng, Z., Hagos, S., Rowe, A. K., Burleyson, C. D., Martini, M. N., & De Szoeke, S. P. (2015). Mechanisms of convective cloud organization by cold pools over tropical warm ocean during the amie/dynamo field campaign. *Journal of Advances in Modeling Earth Systems*, *7*(2), 357–381. https://doi.org/10.1002/2014ms000384

George, G., Stevens, B., Bony, S., Vogel, R., & Naumann, A. K. (2023). Widespread shallow mesoscale circulations observed in the trades. *Nature Geoscience*, *16*(7), 1–6. https://doi.org/10.1038/s41561-023-01215-1

Grant, L. D., Lane, T. P., & Van Den Heever, S. C. (2018). The role of cold pools in tropical oceanic convective systems. *Journal of the Atmospheric Sciences*, *75*(8), 2615–2634. https://doi.org/10.1175/jas-d-17-0352.1

Houze, R. (1994). Cloud dynamics. *International Geophysics*.

Jeevanjee, N., & Romps, D. M. (2015). Effective buoyancy, inertial pressure, and the mechanical generation of boundary layer mass flux by cold pools. *Journal of the Atmospheric Sciences*, *72*(8), 3199–3213. https://doi.org/10.1175/jas-d-14-0349.1

Johnson, R. H., & Ciesielski, P. E. (2013). Structure and properties of madden–julian oscillations deduced from dynamo sounding arrays. *Journal of the Atmospheric Sciences*, *70*(10), 3157–3179. https://doi.org/10.1175/jas-d-13-065.1

Jones, C., & Carvalho, L. M. (2002). Active and break phases in the south american monsoon system. *Journal of Climate*, *15*(8), 905–914. https://doi.org/10.1175/1520-0442(2002)015<0905:aabpit>2.0.co;2

Khairoutdinov, M., & Randall, D. (2006). High-resolution simulation of shallow-to-deep convection transition over land. *Journal of the Atmospheric Sciences*, *63*(12), 3421–3436. https://doi.org/10.1175/jas3810.1

Khairoutdinov, M. F., & Randall, D. A. (2003). Cloud resolving modeling of the arm summer 1997 iop: Model formulation, results, uncertainties, and sensitivities. *Journal of the Atmospheric Sciences*, *60*(4), 607–625. https://doi.org/10.1175/1520-0469(2003)060<0607:crmota>2.0.co;2

Lane, T. P., & Moncrieff, M. W. (2015). Long-lived mesoscale systems in a low–convective inhibition environment. part i: Upshear propagation. *Journal of the Atmospheric Sciences*, *72*(11), 4297–4318. https://doi.org/10.1175/jas-d-15-0073.1

Langhans, W., & Romps, D. M. (2015). The origin of water vapor rings in tropical oceanic cold pools. *Geophysical Research Letters*, *42*(18), 7825–7834. https://doi.org/10.1002/2015gl065623

Madden, R. A., & Julian, P. R. (1971). Detection of a 40–50 day oscillation in the zonal wind in the tropical pacific. *Journal of the Atmospheric Sciences*, *28*(5), 702–708. https://doi.org/10.1175/1520-0469(1971)028<0702:doadoi>2.0.co;2

Madden, R. A., & Julian, P. R. (1972). Description of global-scale circulation cells in the tropics with a 40–50 day period. *Journal of the Atmospheric Sciences*, *29*(6), 1109–1123. https://doi.org/10.1175/1520-0469(1972)029<1109:dogscc>2.0.co;2

Maloney, E. D., & Hartmann, D. L. (2000). Modulation of hurricane activity in the gulf of Mexico by the madden-julian oscillation. *Science*, *287*(5460), 2002–2004. https://doi.org/10.1126/science.287.5460.2002

Moncrieff, M. W. (2019). Toward a dynamical foundation for organized convection parameterization in gcms. *Geophysical Research Letters*, *46*(23), 14103–14108. https://doi.org/10.1029/2019gl085316

Morrison, H., Milbrandt, J., & Milbrandt, J. (2005). Ja curry, and vi khvorostyanov, 2005: A new doublemoment microphysics parameterization for application in cloud and climate models. Part I: Description. *Journal of the Atmospheric Sciences*, *62*(6), 1665–1677. https://doi.org/10.1175/jas3446.1

Nie, J., & Kuang, Z. (2012). Responses of shallow cumulus convection to large-scale temperature and moisture perturbations: A comparison of large-eddy simulations and a convective parameterization based on stochastically entraining parcels. *Journal of the Atmospheric Sciences*, *69*(6), 1936–1956. https://doi.org/10.1175/jas-d-11-0279.1

Riley, E. M., Mapes, B. E., & Tulich, S. N. (2011). Clouds associated with the Madden–Julian oscillation: A new perspective from cloudsat. *Journal of the Atmospheric Sciences*, *68*(12), 3032–3051. https://doi.org/10.1175/jas-d-11-030.1

Rotunno, R., Klemp, J. B., & Weisman, M. L. (1988). A theory for strong, long-lived squall lines. *Journal of the Atmospheric Sciences*, *45*(3), 463–485. https://doi.org/10.1175/1520-0469(1988)045<0463:atfsll>2.0.co;2

Ruppert, J. H., & Johnson, R. H. (2015). Diurnally modulated cumulus moistening in the preonset stage of the madden–Julian oscillation during dynamo. *Journal of the Atmospheric Sciences*, *72*(4), 1622–1647. https://doi.org/10.1175/jas-d-14-0218.1

Sakaeda, N., Kiladis, G., & Dias, J. (2020). The diurnal cycle of rainfall and the convectively coupled equatorial waves over the maritime continent. *Journal of Climate*, *33*(8), 3307–3331. https://doi.org/10.1175/jcli-d-19-0043.1

Sakaeda, N., & Torri, G. (2022). The behaviors of intraseasonal cloud organization during dynamo/amie. *Journal of Geophysical Research: Atmospheres*, *127*(7), e2021JD035749. https://doi.org/10.1029/2021jd035749

Sakaeda, N., & Torri, G. (2023). The observed effects of cold pools on convection triggering and organization during dynamo/amie. *Journal of Geophysical Research: Atmospheres*, *128*(17), e2023JD038635. https://doi.org/10.1029/2023jd038635

Schlemmer, L., & Hohenegger, C. (2014). The formation of wider and deeper clouds as a result of cold-pool dynamics. *Journal of the Atmospheric Sciences*, *71*(8), 2842–2858. https://doi.org/10.1175/jas-d-13-0170.1

Shamekh, S., Lamb, K. D., Huang, Y., & Gentine, P. (2023). Implicit learning of convective organization explains precipitation stochasticity. *Proceedings of the National Academy of Sciences*, *120*(20), e2216158120. https://doi.org/10.1073/pnas.2216158120

Stevens, B., Bony, S., Brogniez, H., Hentgen, L., Hohenegger, C., Kiemle, C., et al. (2020). Sugar, gravel, fish and flowers: Mesoscale cloud patterns in the trade winds. *Quarterly Journal of the Royal Meteorological Society*, *146*(726), 141–152. https://doi.org/10.1002/qj.3662

Tang, M. (2024). Data for "The role of cold pools in modulating convective organization during the MJO. *Zenodo*. https://doi.org/10.5281/zenodo.10939337

Tompkins, A. M. (2001). Organization of tropical convection in low vertical wind shears: The role of cold pools. *Journal of the Atmospheric Sciences*, *58*(13), 1650–1672. https://doi.org/10.1175/1520-0469(2001)058<1650:ootcil>2.0.co;2

Tompkins, A. M., & Semie, A. G. (2017). Organization of tropical convection in low vertical wind shears: Role of updraft entrainment. *Journal of Advances in Modeling Earth Systems*, *9*(2), 1046–1068. https://doi.org/10.1002/2016ms000802

Torri, G., & Kuang, Z. (2016a). A Lagrangian study of precipitation-driven downdrafts. *Journal of the Atmospheric Sciences*, *73*(2), 839–854. https://doi.org/10.1175/jas-d-15-0222.1

Torri, G., & Kuang, Z. (2016b). Rain evaporation and moist patches in tropical boundary layers. *Geophysical Research Letters*, *43*(18), 9895–9902. https://doi.org/10.1002/2016gl070893

Torri, G., & Kuang, Z. (2019). On cold pool collisions in tropical boundary layers. *Geophysical Research Letters*, *46*(1), 399–407. https://doi.org/10.1029/2018gl080501

Torri, G., Kuang, Z., & Tian, Y. (2015). Mechanisms for convection triggering by cold pools. *Geophysical Research Letters*, *42*(6), 1943–1950. https://doi.org/10.1002/2015gl063227

Wang, B., Webster, P. J., & Teng, H. (2005). Antecedents and self-induction of active-break south asian monsoon unraveled by satellites. *Geophysical Research Letters*, *32*(4). https://doi.org/10.1029/2004GL020996

Wang, S., Sobel, A. H., Zhang, F., Sun, Y. Q., Yue, Y., & Zhou, L. (2015). Regional simulation of the October and November mjo events observed during the Cindy/dynamo field campaign at gray zone resolution. *Journal of Climate*, *28*(6), 2097–2119. https://doi.org/10.1175/jcli-d-14-00294.1

Wing, A. A., & Emanuel, K. A. (2014). Physical mechanisms controlling self-aggregation of convection in idealized numerical modeling simulations. *Journal of Advances in Modeling Earth Systems*, *6*(1), 59–74. https://doi.org/10.1002/2013ms000269

Yang, Q., Majda, A. J., & Moncrieff, M. W. (2019). Upscale impact of mesoscale convective systems and its parameterization in an idealized gcm for an mjo analog above the equator. *Journal of the Atmospheric Sciences*, *76*(3), 865–892. https://doi.org/10.1175/jas-d-18-0260.1

Zhang, C. (2005). Madden-julian oscillation. *Reviews of Geophysics*, *43*(2). https://doi.org/10.1029/2004RG000158

Zhang, Y., & Klein, S. A. (2010). Mechanisms affecting the transition from shallow to deep convection over land: Inferences from observations of the diurnal cycle collected at the arm southern great plains site. *Journal of the Atmospheric Sciences*, *67*(9), 2943–2959. https://doi.org/10.1175/2010jas3366.1

Zuidema, P., Torri, G., Muller, C., & Chandra, A. (2017). A survey of precipitation-induced atmospheric cold pools over oceans and their interactions with the larger-scale environment. *Surveys in Geophysics*, *38*(6), 1283–1305. https://doi.org/10.1007/s10712-017-9447-x

References From the Supporting Information

Skamarock, W. C., Klemp, J. B., Dudhia, J., Gill, D. O., Barker, D. M., Duda, M. G., et al. (2008). A description of the advanced research WRF version 3. *NCAR Technical Note*, *475*, 113.